- Technical Paper -

EXPERIMENTAL AND ANALYTICAL EVALUATIONS OF ASR-INDUCED DAMAGE

Yulong ZHENG[*1], Kenji KOSA[*2], Nobuo UEHARA[*3]

ABSTRACT

To estimate the behavior of stirrup, which is significant for the fracture around stirrup due to ASR, specimen with expansive mortar cast into the frame of ordinary concrete is conducted. The ASR-induced circular and elongated deformation as 5.00mm and 3.33mm are generated by the bending and tensile action. Besides, angular increment about 2.0° is verified for corner concrete. This is responsible for the opening deformation of stirrup, being crucial for progress of initial damage until to fracture. By FEM analysis, external deformations in experiment are generally reproduced.

Keywords: ASR, simulation experiment, FEM analysis, stirrup fracture, deformations

1. INTRODUCTION

For recent years, due to the Alkali Silica Reaction, (ASR for short), many concrete structures suffered degradations. It is reported that caused by the inner expansion of ASR, the bent parts of reinforcing stirrups in bridge beam are frequently fractured [1]. As one of the inferred fracture mechanisms of stirrup, it is verified that initial cracks are generated during the bending operation for bent part of stirrup. Thus, induced by the inner expansion, stirrup would have angular increment which promotes the progress of initial cracks till to fracture. To confirm the behavior of stirrup together with the external deformations, experimental tests and FEM analysis are attempted.

Besides, caused by ASR, deterioration of concrete as reduction of compressive strength and young's modulus is occurred. However, aiming at evaluating the influence from inner expansion on external deformation behavior, which is much relative to movement of stirrup, experimental tests are conducted. Therefore, specimens with expansive mortar cast into the frame of ordinary concrete are made. The general forms of external deformations produced by the inner expansion is studied over time; after that, the characteristics of deformation is evaluated through classification; further, induced by the external deformation, the movement of corner concrete concerning the stirrup fracture is investigated. In addition, FEM analysis is conducted for giving verification to experimental results.

2. EXPERIMENTAL CONDITIONS

In this chapter, the experimental conditions including the specimen condition and the measurement method for external degradations will be introduced.

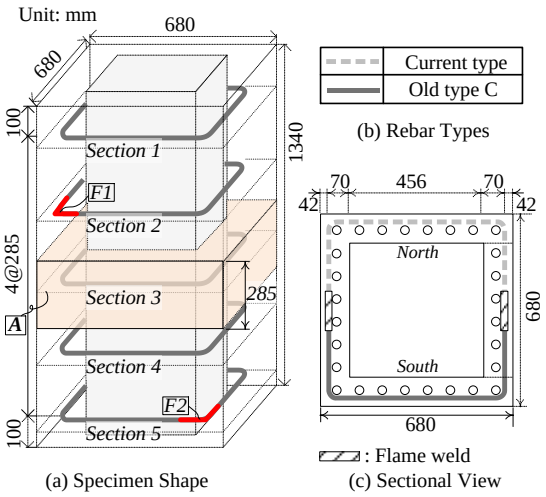

Fig. 1 Specimen conditions

2.1 Specimen Condition

Fig. 1 illustrates the shapes and reinforcements of the specimen. For sake of simulating the effect from inner ASR expansion on external degradations and stirrups, the expansive mortar is cast in the square hollow by using ordinary concrete as frame. The external size is 680mm×680mm×1340mm with cross section to be 1/4 of that for the actual bridge beam with stirrups fractured. Besides, the dimension of expansive mortar is set as 456mm×456mm. The spacing of stirrups is 285mm giving the stirrup ratio as 0.22% which equals to that of the actual bridge beam. As illustrated in Fig. 1-(b), stirrups adopt the D16 rebar with one type using the rib shape based on the current specification (‘current type’ for short) and another type using the bamboo joint rib (ribs that are aligned in parallel with spacing) based on the old specification (‘old type C’ for short). More details for different rebar types can be referred to former research [2]. In addition,

*1 Doctoral Student, Dept. of Civil Engineering, Kyushu Institute of Technology, JCI Student Member
*2 Ph.D., Prof., Dept. of Civil Engineering, Kyushu Institute of Technology, JCI Member
*3 Cement / Concrete Research Laboratory, Sumitomo Osaka Cement Co., Ltd. JCI Member

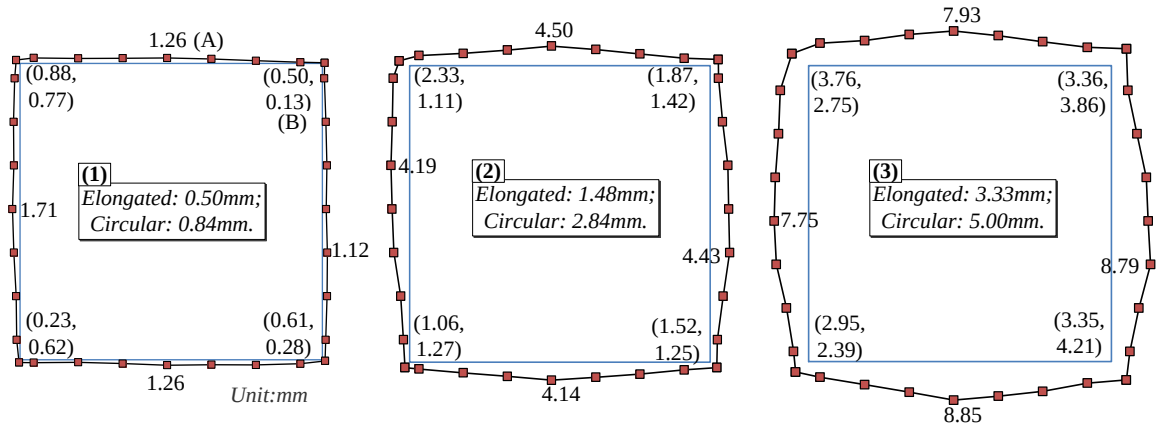

(a) After 8.0hr (b) After 10.0hr (c) After 24.0hr (Final)

Fig. 3 Time variation of deformation forms

the image of cross section is shown in Fig. 1-(c). Since it is limited for the length of old type rebar which are chipped out from the actual bridge beam, two types of stirrups are connected using flame weld (Fig. 1-(c)).

The detail about mix proportions used for the frame concrete and the expansive mortar is referred from [2]. The frame concrete uses the strength as 27N/mm^2 being the design strength for the actual bridge beam. By cylinder tests, the real strength is obtained as 35N/mm^2. Besides, the lime type expansive agent is set as 200kg/m^3 to simulate the severe degradation condition. To avoid the influence from sun exposure, the specimen was set up in indoor condition.

2.2 Measurement Method

For studying the deformation conditions in the cross sections of stirrups, Fig. 2 illustrates the measuring method. All 5 cross sections with stirrups arranged are the measuring objects. As shown in Fig. 2-(a), for measuring deformations of the specimen, fixed frame is set around each cross section. To obtain the length from fixed frame to the concrete surface, measuring scale is set in the fixed frame at the position 40mm away from endpoint of the corner and then followed by each 100mm (refer to Fig. 2-(b)). From calculating the difference value of lengths before and after expansion, the deformation can be obtained. Moreover, it is considered that deformation is composed of elongated deformation and circular deformation. For instance, the deformation A (vertical displacement from a_1 to a_2, Fig. 2-(b)) in corner point is defined as the elongated deformation; while the difference between the maximum deformation B (vertical displacement from b_1 to b_2, Fig. 2-(b)) and the deformation A is defined as circular deformation.

3. EXTERNAL DEFORMATIONS

Features of external deformations produced by the inner expansion are discussed in this chapter. At first, the general deformation condition of specimen is studied; thus, the classified deformations are evaluated; afterwards, induced by the external deformations, the

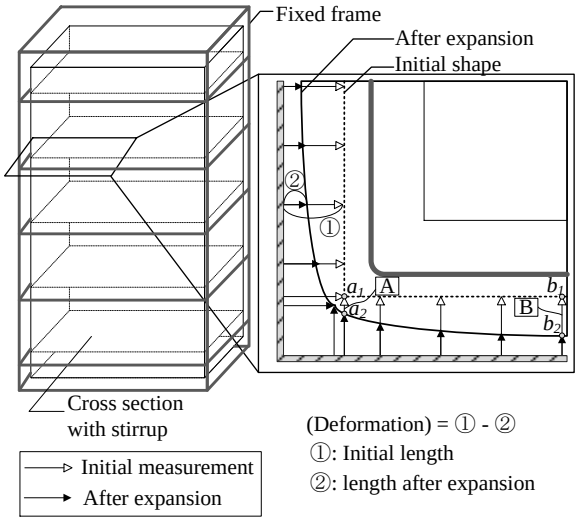

(a) Positions for Measurement (b) Method for Measurement

Fig. 2 Measurement method

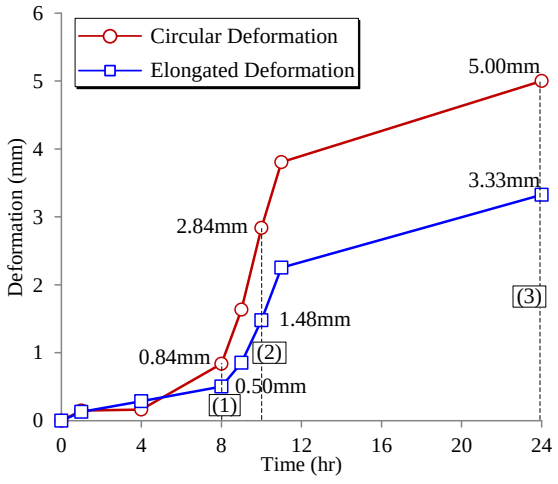

Fig. 4 Time variation of elongated/circular deformations

movement of corner concrete is also investigated.

3.1 General Deformation Forms

For studying the development of deformations along with expansion, the time variations are presented in Fig. 3. After 8.0hr of expansion, the deformation shape is shown in Fig. 3-(a). The values in profile (like A in Fig. 3-(a)) represents the maximum deformation of each profile; while the values in corners (like B) means the deformations in x and y direction of corner points.

Thus, combined with the definitions illustrated in Fig. 2, the general elongated deformation is computed as 0.50mm (average of 8 deformation values in corners of Fig. 3-(a)). Further, the average circular deformation is 0.84mm (circular deformation is 0.81, 0.56, 0.81 and 1.16mm for south, east, north and west profile, respectively). Besides, it is attained that the maximum deformation is 1.71mm and 0.88mm for center and corner of profile, respectively. When after 10.0hr of expansion (Fig. 3-(b)), the general deformations have been expanded with maximum value in center as 4.50mm while in corner varies to be 2.33mm. The elongated and circular deformation has increased to be 1.48mm and 2.84mm, respectively. At last, for the final state when after 24.0hr (Fig. 3-(c)), the general deformation has further increment with maximum values change to be 8.85mm and 4.21mm in center and corner of profile, respectively. Besides, the elongated deformation increases to be the maximum as 3.33mm and the circular deformation as 5.00mm.

3.2 Evaluation of Classified Deformations

Herein, concerning on the time variation of classified deformations, Fig. 4 illustrates the data for each time point. Points (1), (2) and (3) in Fig. 4 are corresponding with those in Fig. 3. The circular deformation increases slowly before 8.0hr ((1) of Fig. 4) with 0.84mm. Thus, intense raise occurs via 10.0hr ((2)) as 2.84mm. After 11.0hr, increment of deformation begins to decreasing. Expansion is supposed to converge with the maximum as 5.00mm ((3)). Similarly, elongated deformation also has smaller increase before 8.0hr as 0.50mm and then dramatic growth by 10.0hr as 1.48mm. After 11.0hr, slight raise occurs with the maximum 3.33mm. In summary, it is clarified that elongated and circular deformations are produced along with the inner expansion.

Further, the mechanisms for generation of elongated and circular deformation are discussed. Distributed load is assumed to act on the frame concrete. The frame part *AB* (Fig. 5-(a)) is concentrated and assumed to receive fixed restrains in two ends. Thus, the distributed load in the vertical direction w_y produces moment (*M*) with the distribution image shown in Fig. 5-(b); the corresponding maximum displacement δ_m is generated in the central frame due to the bending rigidity. Further, the distributed load in horizontal direction w_x transmit to the part AB to produce the axial force (*N*) with the uniform distribution referred to Fig. 5-(b); similarly, the deformation δ_n is produced from

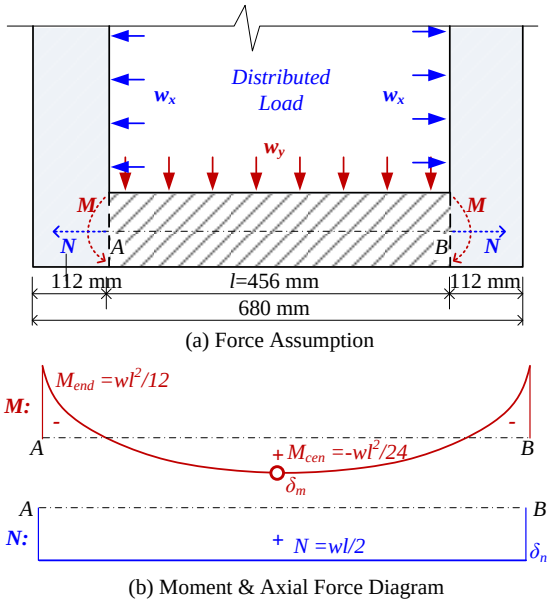

Fig. 5 Mechanism for generation of deformations

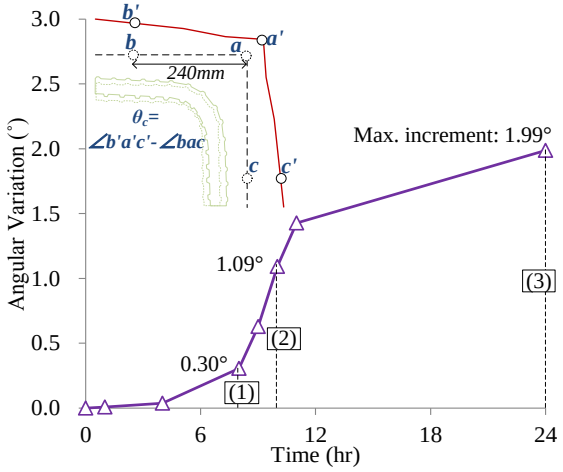

Fig. 6 Angular variation of corner concrete

the tensile rigidity. Therefore, it is considered that the circular and the elongated deformation is correlated with δ_m and δ_n, which is generated from bending and tensile effect, respectively.

3.3 Movement of Corner Concrete

For confirming the fracture mechanism of stirrups, the movement behavior of corner concrete is considered to be significant. Thus, as illustrated in Fig. 6, there points *bac* with the spacing value *ab* and *ac* as 240mm are selected at the corner. The angular variations of *bac* (θ_c) in four corners of specimen is averaged for evaluation due to their small difference. As presented in Fig. 6, the angular change has similar variation trend to deformations (refer to Fig. 4); smaller rise is confirmed before 8.0hr ((1) of Fig. 6) with the value to be 0.30°; thus, drastic variation generates through 10.0hr ((2)) with the value as 1.09°; after 11.0hr, the value raise slowly with the maximum to be 1.99° in 24.0hr ((3)). From the positive angular

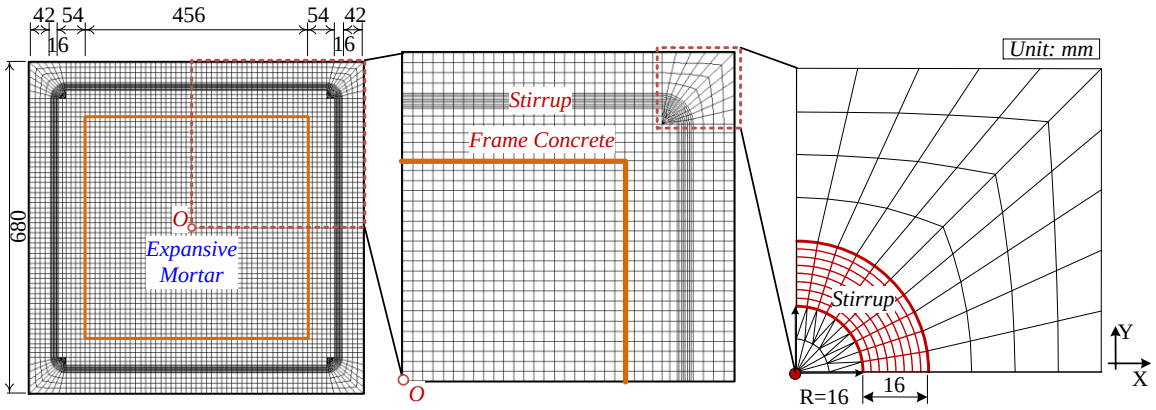

(a) Analysis Model (b) Enlarge of 1/4 Part (c) Bent Part of Stirrup

Fig. 7 Analytical model

variations, the corner concrete is verified to have opening deformation caused by the general circular deformation. Further, the stirrup is estimated to have the similar opening deformation, which is considered to be crucial for the progress of initial damage in inner stirrup till to fracture. Moreover, two fractures *F1* and *F2* (Fig. 1-(a)) are confirmed in bent part of stirrups.

4. ANALYTICAL CONDITIONS & RESULTS

For reproducing the experiment, FEM analysis is carried out. The analytical conditions are explained firstly; thus, the results are compared with experiment.

4.1 Analytical and Material Model

The 2-dimensional elastic-plastic finite element analysis is conducted. The whole section is used for modeling as presented in Fig. 7-(a). The expansive mortar with the size as 456mm×456mm is simulated. Referring to the former Fig. 1-(a), the spacing of stirrups for section 2~4 is same as 285mm. Thus, for modeling these three sections, one stirrup is input into the model with depth of the concrete model as 285mm (refer to A of Fig. 1-(a) for image, section 3 for instance). Based on observations from experiment, expansion in axial direction is also confirmed. Therefore, four-node quadrilateral isoparametric plane stress elements considering strain in three directions are applied. Besides, point *O* (Fig. 7-(a)) is fixed in *x*, *y* directions to avoid the shift of the central point. For simulating the bent part of stirrup in detail, plane stress elements are also applied to stirrup (Fig. 7-(c)) with the width as 16mm (diameter) and the depth as 12.4mm (to result the same area to D16 as 198.6mm^2).

Fig. 8-(a) presents the stress-strain model of frame concrete. In compression side, the para-curve is developed until the compressive strength as 35N/mm^2. The Drucker-Prager criterion is used for the biaxial compressive situation. With respect to the tensile side, the curve grows in linear to the tensile strength. Then considering the softening condition, 1/4 model is used. Besides, the Rankine criterion is applied. Fig. 8-(b) describes the stress-strain model for stirrup. The yield and tensile strength is based on the values obtained by

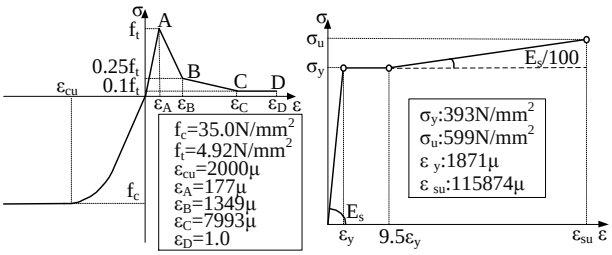

(a) Frame Concrete (b) Steel

Fig. 8 Stress-strain for frame concrete/steel

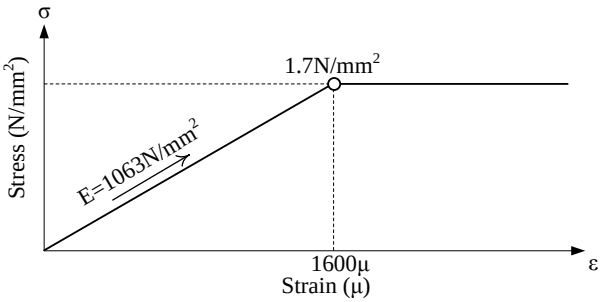

Fig. 9 Stress-strain for expansive mortar

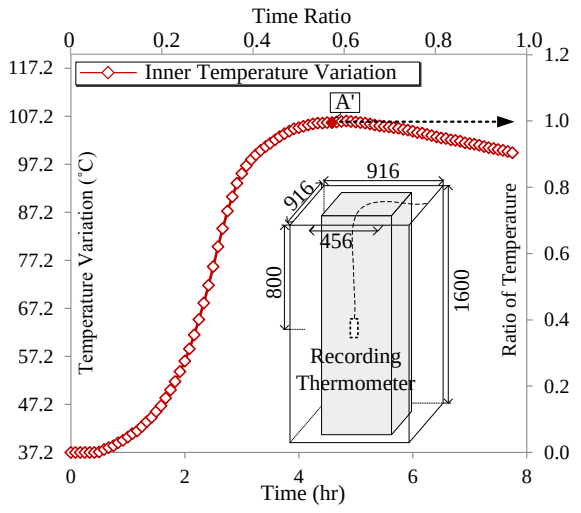

Fig. 10 Input of expansive strain

tensile test. Further, Von-Mises criterion is adopted.

For the expansive mortar, the basic bi-linear stress-strain curve is settled (Fig. 9). In the former research [3], compressive tests were conducted for expansive concrete which was in hardening status after 35 days' curing. The strength and corresponding strain are obtained as around 17N/mm^2 and 1600μ with the elastic modulus as 10625N/mm^2. During the process for actual hydration reaction of expansive agent, these factors are considered to be smaller. Further, as the expansive agent is confirmed to have liquid behavior [4], analysis using 1/10 of the elastic modulus and the strength shown above is selected for evaluation herein.

Besides, to simulate time depended expansion in the model, the inner temperature of the serial specimen with same size of expansive mortar is used. As presented in Fig. 10, before expansion, a recording thermometer is placed in the central point of the cross-section located in middle of the specimen. The time variation of recorded temperature is dimensionless and used for the time variation of thermal expansion acting on the model of expansive mortar (Fig. 7). The coefficient of expansion as 1.0×10^{-5} /°C is applied to produce the maximum free expansive strain 30000μ from research [5] (based on free expansive strains of cases using the same type of expansive agent and the same water/powder ratio). Strain is set constantly after maximum (A' in Fig. 10) for convergence in analysis.

4.2 Evaluation of Results

Based on the analytical conditions described above, the corresponding results are evaluated. Fig. 11 illustrates the external deformation conditions. It is noted that from 8.0hr to 24.0hr of expansion, the deformation in center increases from 4.34mm to 7.35mm, greater than 1.59mm to 2.69mm of those in corner. The similar circular deformation to experiment is verified. Besides, applying the identical definitions to experiment, the comparison of elongated deformation is illustrated in Fig. 12. It is noted that similar time variation trend is generated for experiment and analysis. However, regarding the difference of deformations in point (1) and (2) (Fig. 12), variation of deformation from experiment seems to have a small time lag compared with analysis which is based on the time variation of inner temperature. This time lag can also be inferred based on the test of expansive agent [6].

Besides, the comparison of circular deformation is presented in Fig. 13. Similar time variation trend is obtained compared with the experiment. The maximum circular deformation is obtained as 4.66mm in analysis closing to 5.00mm of the experiment. Simultaneously, from Fig. 14, angular change of corner concrete is also confirmed by analysis with the maximum increment as 1.80° near to 1.99° of the experiment.

In addition, to confirm the generation mechanism of deformations explained in previous chapter, the strain distribution of frame concrete is studied. After 24.0hr, the maximum principle strain in the central frame of the 1/4 cross-section is illustrated in Fig. 15. Great strains mainly generate in 5 sections (A to E)

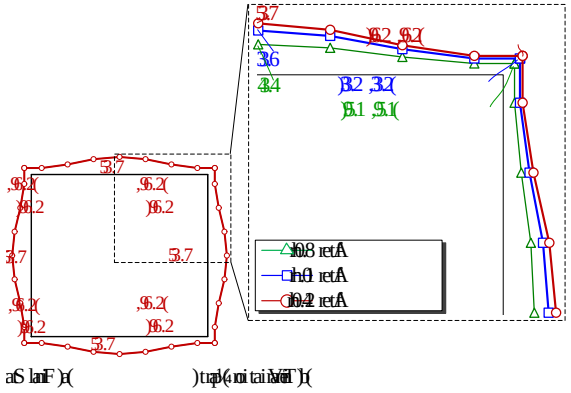

Fig. 11 Time variation of deformation forms (analysis)

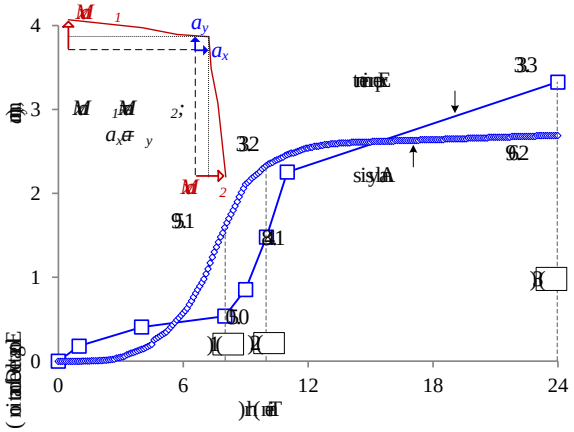

Fig. 12 Time variation of elongated deformation

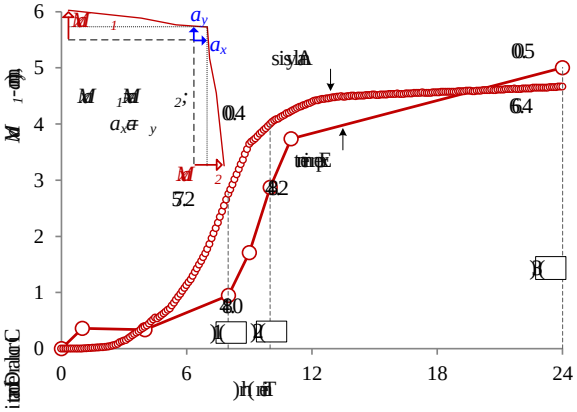

Fig. 13 Time variation of circular deformation

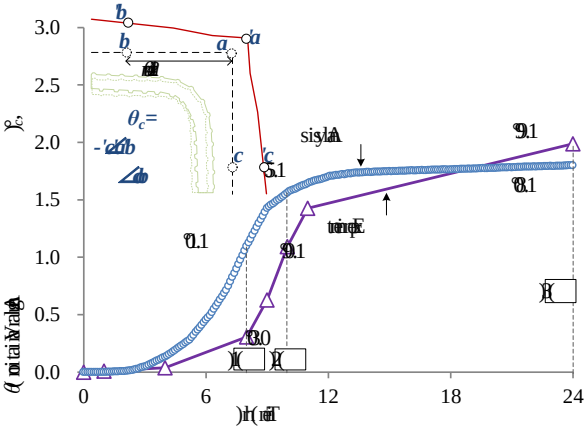

Fig. 14 Time variation of angular change

which infers occurrences of cracks. For evaluating numerically, the detailed strain distributions in *x* direction of the sections are plotted. For sections A to C, it is noted that strains are divided by two parts as those from tensile and bending effect. For sections D and E, similar form is confirmed while the strain from bending in the upper section is negative due to the minus moment in corner part (refer to point B of Fig. 5-(b)).

Further, the strains from tensile effect in the 5 sections are summed to be 0.251 (0.0557 for *A*, 0.0278 for *B*, 0.0553 for *C*, 0.0487 for *D* and 0.0630 for *E*). From the product of the summed strain and equivalent length (determined as 10mm based on element size), it is obtained that deformation from tensile effect is 2.51mm which is close to the elongated deformation as 2.69mm. Therefore, combined with the estimation in the former Fig. 5, caused by the inner expansion, tensile and bending effects both generate. Further, it is confirmed that tensile effect produce the elongated deformation while bending effect would give the occurrence of circular deformation.

Afterwards, the circular deformation is considered to simultaneously cause corner concrete to have opening deformation, which is estimated to produce the angular increment in the bent part of stirrup. Therefore, the initial damage in the stirrup is estimated to progress for inducing the fracture occurs.

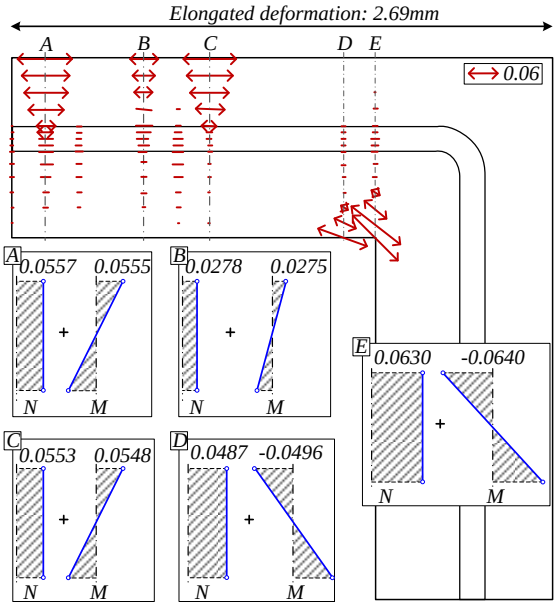

Fig. 15 Strain distributions in frame concrete

5. CONCLUSIONS

To estimate the stirrup movement, which is significant for the fracture around stirrup due to ASR, experimental tests and FEM analysis are conducted. Specimen with expansive mortar cast into the frame of ordinary concrete is made. Through classification, characteristics of external deformation is evaluated. Further, the movement of corner concrete concerning the stirrup fracture is investigated. At last, FEM analysis is performed for verifying experimental result and the generating mechanism. Therefore, the following conclusions can be obtained:

(1) During the experiment, the evolution of deformations in specimen is recorded. It is found that for the ultimate state, maximum deformation around 9.0mm occurs in center of profiles for the specimen. The specimen is confirmed to have the general ASR-induced circular deformation.
(2) From experimental results, deformation is classified as circular deformation caused by bending effect and elongated deformation from tensile effect in detail. It is clarified that both two kinds of deformations generate along with the inner expansion with the maximum occurred at 24 hours of expansion and the values to be 5.00mm and 3.33mm for circular and elongated deformation, respectively.
(3) Based on the experiment, for estimating the behavior of stirrups, movement of corner concrete is studied. It is confirmed that together with the circular deformation, corner concrete produces opening deformation along with expansion with the maximum angular increment as 1.99°. This is estimated to produce the opening deformation with angular increment in the bent part of stirrup. Hence, the initial damage in the stirrup is progressed until to fracture.
(4) For the FEM analysis, the circular and elongated deformation has similar time variation to experiment with the maximum to be 4.66 and 2.69mm, respectively. The angular increment is also verified to be 1.80° for the ultimate. From the study of strain distribution in frame concrete, the strain from tensile effect results the deformation as 2.51mm closing to the elongated deformation; while it is also considered that strain from bending effect would produce the circular deformation.

REFERENCES

[1] JSCE: "Report of Committee for ASR Countermeasures -Fracture of Rebar and New Correspondence," Concrete Library, No. 124, 2005, pp.1-2~1-77.
[2] Kosa, K. et al. "Evaluation of Deterioration Using an ASR-imitated Test Specimen," Journal of JSCE, Ser. E2, Vol. 69, No. 2, 2013, pp. 166-181.
[3] Okamura, H. and Tsuji, Y. "Behavior of Chemically Prestressed Concrete Member," Proceedings of JSCE, No. 225, 1974, pp. 101-108.
[4] Harada, T., Idemitsu, T. and Watanabe, A. "Demolition of Concrete with Expansive Demolition Agent," Journal of JSCE, No. 360/V-3, 1985, pp. 61-70.
[5] KABSE: "Performance of Expansive Materials and its Application," 1999, pp.30~33.
[6] Harada, T. and Matuda, H. "The Connecting Method of Prestressed Concrete Members by Using Chemical Jack with Expansive Demolition Agent," Proceedings of the JCI, Vol.14, No.1, 1992, pp. 177-182.